THE JOURNAL OF BIOLOGICAL CHEMISTRY
Vol. 279, No. 11, Issue of March 12, pp. 10784–10795, 2004

Printed in U.S.A.

Human Cytosolic 3α-Hydroxysteroid Dehydrogenases of the Aldo-keto Reductase Superfamily Display Significant 3β-Hydroxysteroid Dehydrogenase Activity

IMPLICATIONS FOR STEROID HORMONE METABOLISM AND ACTION*

Received for publication, December 5, 2003
Published, JBC Papers in Press, December 12, 2003, DOI 10.1074/jbc.M313308200

Stephan Steckelbroeck, Yi Jin, Sridhar Gopishetty, Busola Oyesanmi, and Trevor M. Penning‡

From the Department of Pharmacology, University of Pennsylvania School of Medicine, Philadelphia, Pennsylvania 19104-6084

The source of NADPH-dependent cytosolic 3β-hydroxysteroid dehydrogenase (3β-HSD) activity is unknown to date. This important reaction leads *e.g.* to the reduction of the potent androgen 5α-dihydrotestosterone (DHT) into inactive 3β-androstanediol (3β-Diol). Four human cytosolic aldo-keto reductases (AKR1C1–AKR1C4) are known to act as non-positional-specific 3α-/17β-/20α-HSDs. We now demonstrate that AKR1Cs catalyze the reduction of DHT into both 3α- and 3β-Diol (established by ^{1}H NMR spectroscopy). The rates of 3α-*versus* 3β-Diol formation varied significantly among the isoforms, but with each enzyme both activities were equally inhibited by the nonsteroidal anti-inflammatory drug flufenamic acid. *In vitro*, AKR1Cs also expressed substantial 3α[17β]-hydroxysteroid oxidase activity with 3α-Diol as the substrate. However, in contrast to the 3-ketosteroid reductase activity of the enzymes, their hydroxysteroid oxidase activity was potently inhibited by low micromolar concentrations of the opposing cofactor (NADPH). This indicates that *in vivo* all AKR1Cs will preferentially work as reductases. Human hepatoma (HepG2) cells (which lack 3β-HSD/Δ$^{5-4}$ ketosteroid isomerase mRNA expression, but express AKR1C1–AKR1C3) were able to convert DHT into 3α- and 3β-Diol. This conversion was inhibited by flufenamic acid establishing the *in vivo* significance of the 3α/3β-HSD activities of the AKR1C enzymes. Molecular docking simulations using available crystal structures of AKR1C1 and AKR1C2 demonstrated how 3α/3β-HSD activities are achieved. The observation that AKR1Cs are a source of 3β-tetrahydrosteroids is of physiological significance because: (i) the formation of 3β-Diol (in contrast to 3α-Diol) is virtually irreversible, (ii) 3β-Diol is a pro-apoptotic ligand for estrogen receptor β, and (iii) 3β-tetrahydrosteroids act as γ-aminobutyric acid type A receptor antagonists.

Two classes of 3β-hydroxysteroids, *i.e.* the Δ^5-3β-hydroxysteroids and the fully saturated 3β-tetrahydrosteroids, represent pivotal intermediates in steroid hormone metabolism. In steroidogenic glands, Δ^5-3β-hydroxysteroid precursors are converted into Δ^4-3-ketosteroids to produce active steroid hormones (1, 2), whereas 3-ketosteroid reduction of 5α/5β-dihydrosteroids into 3β-tetrahydrosteroids is an important catabolic step in steroid hormone transformation.

Human steroid hormone target tissues like the prostate express membrane attached and/or cytosolic 3α-HSD[1] and 3β-HSD activity (3–9). One key example of the catabolic function of these HSDs is the 3-ketosteroid reduction of the potent androgen 5α-dihydrotestosterone (DHT, 17β-hydroxy-5α-androstan-3-one) into the inactive androgens 5α-androstane-3α,17β-diol (3α-Diol; Fig. 1) and 5α-androstane-3β,17β-diol (3β-Diol) (10–12). *In vivo*, the formation of 3β-Diol is virtually irreversible, whereas 3α-Diol can be converted back to DHT via 3α-hydroxysteroid oxidase activity (13–17). Reformation of DHT from 3β-Diol is prevented, because 3β-Diol is either irreversibly hydroxylated at the C-6 and/or C-7 position or is oxidized to (epi)androsterone (13–20). 3α-Diol and 3β-Diol, once formed, are also glucuronidated and sulfated, leading to elimination of the androstanes into the circulation and their final excretion (21, 22).

In humans, the irreversible NAD^+-dependent conversion of Δ^5-3β-hydroxysteroid into Δ^4-3-ketosteroids is catalyzed by two members of the short chain dehydrogenase/reductase (SDR) family: the bifunctional 3β-HSD/Δ$^{5-4}$ ketosteroid isomerase (3β-HSD/KSI) isoforms type 1 and type 2, which express 3β-HSD and isomerase activity in a single protein (1, 2, 23). Besides their essential role in the formation of active steroid hormones, the 3β-HSD/KSI isoforms also catalyze the NAD(H)-dependent *in vitro* interconversion of 3-keto- and 3β-hydroxy-5α-androstanes (24, 25). However, *in vivo* their directionality will be governed by the redox environment and, under normal cofactor ratios (were NAD^+ dominates over NADH) (26, 27), they will work preferentially as oxidases. Moreover, the 3β-HSD/KSI isoforms are membrane-associated and, therefore, cannot be the source of the cytosolic NADPH-dependent 3β-HSDs in target tissues capable of producing 3β-tetrahydrosteroids.

Proteins of two phylogenies catalyze the 3-ketosteroid reduction of 5α/5β-dihydrosteroids via 3α-HSD activity: (i) four cytosolic enzymes of the AKR1C subfamily in the aldo-keto re-

* This work was supported by Grants DK47015 and CA90744 (to T. M. P.) from the National Institutes of Health. The costs of publication of this article were defrayed in part by the payment of page charges. This article must therefore be hereby marked "*advertisement*" in accordance with 18 U.S.C. Section 1734 solely to indicate this fact.

‡ To whom correspondence should be addressed: Dept. of Pharmacology, University of Pennsylvania School of Medicine, 130C John Morgan Bldg., 3620 Hamilton Walk, Philadelphia, PA 19104-6084. Tel.: 215-898-9445; Fax: 215-573-2236; E-mail: penning@pharm.med.upenn.edu.

[1] The abbreviations used are: HSD, hydroxysteroid dehydrogenase; AKR, aldo-keto reductase; $CDCl_3$, deuterated chloroform; DHT, 17β-hydroxy-5α-androstane-3-one; 3α(β)-Diol, 5α-androstane-3α(β),17β-diol; $GABA_A$ receptor, γ-aminobutyric acid type A receptor; HepG2, human hepatoma cell line; NSAID, nonsteroidal anti-inflammatory drug; PDB, Protein Data Bank; RT, reverse transcription; SDR, short chain dehydrogenase/reductase; RoDH, retinol dehydrogenase type 4; KSI, Δ$^{5-4}$ ketosteroid isomerase.

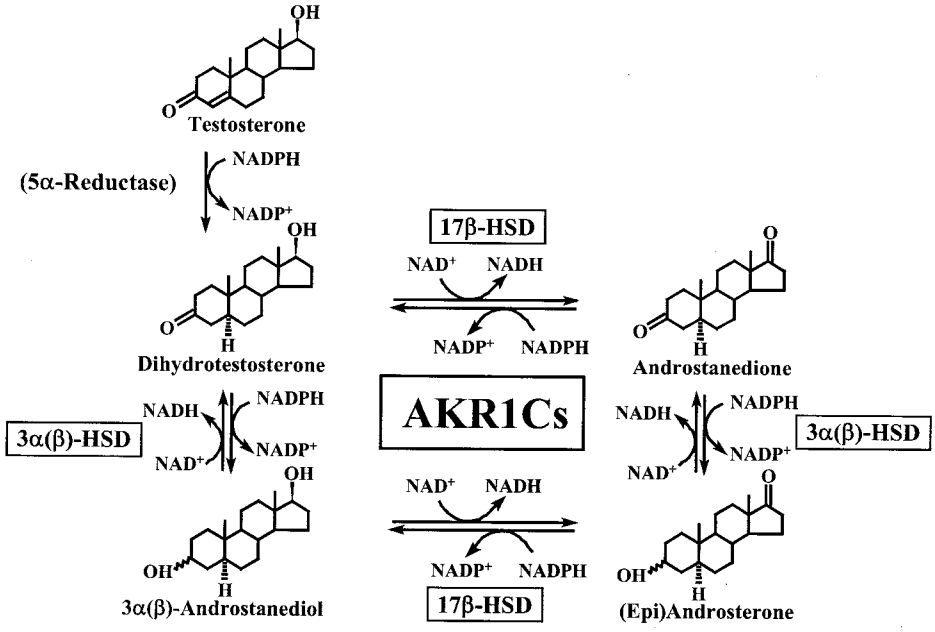

FIG. 1. **Role of human AKR1C isoforms in androgen metabolism.** Human AKR1C1–AKR1C4 are known to catalyze *in vitro* the bidirectional interconversion of 3-ketosteroids with 3α-hydroxysteroids, as well as 17-ketosteroids with 17β-hydroxysteroids.

ductase (AKR) superfamily, *i.e.* 20α[3α]-HSD (AKR1C1), human 3α-HSD type 3 (AKR1C2; also known as bile acid-binding protein), human 3α-HSD type 2 (AKR1C3; also known as human 17β-HSD type 5), and human 3α-HSD type 1 (AKR1C4) (2) and (ii) five membrane-associated enzymes of the SDR family, *i.e.* 11-*cis*/9-*cis*-retinol dehydrogenase, retinol dehydrogenase type 4 (RoDH-4), "human RoDH" or RoDH-like 3α-HSD, "novel type human microsomal 3α-HSD" and short chain L-3-hydroxyacyl-CoA dehydrogenase (28–33).

Previously, AKR1C1–AKR1C4 have been shown to act as non-positional-specific 3α-/17β-/20α-HSDs (34). This means that *in vitro* these isoforms catalyzed the bi-directional interconversion of 3-ketosteroids and 3α-hydroxysteroids, 17-ketosteroids, and 17β-hydroxysteroids, as well as 20-ketosteroids and 20α-hydroxysteroids to varying extents. However, their retention of stereo-specificity has not been addressed to date. Using more discriminating TLC systems than that previously utilized (34), we now demonstrate for the first time that *in vitro* as well as *in vivo* AKR1C1–AKR1C4 catalyze the reduction of DHT not only into 3α-Diol but also into 3β-Diol. The ratio of reductive 3α-HSD *versus* 3β-HSD activity varied significantly among the isoforms in a way that AKR1C1 has to be considered as a 3β-HSD with subsidiary 3α-HSD activity, AKR1C2 as an efficient and an almost exclusive 3α-HSD, AKR1C3 as a weak 3α/3β-HSD, and AKR1C4 as an efficient 3α-HSD with subsidiary 3β-HSD activity. Inhibition experiments using the nonsteroidal anti-inflammatory drug (NSAID) flufenamic acid (which acts as a competitive inhibitor) indicated that a single active site is responsible for the formation of the diastereomers. We provide evidence that *in vivo* all isoforms will work predominantly as reductases and show that 3β-HSD activity of the AKR1C isoforms is biologically relevant in human hepatoma cells. Using available crystal structures of AKR1C1 and AKR1C2 (35–37), we employed molecular docking to explain why the former functioned predominantly as a 3β-HSD and the latter as a 3α-HSD. Thus, the human AKR1C isozymes are both non-positional and non-stereo-selective HSDs and represent a potential cytosolic source of 3β-tetrahydrosteroids in target tissues such as prostate and brain.

EXPERIMENTAL PROCEDURES

Steroids and Chemicals—[4-^{14}C]DHT (53.5 mCi/mmol) and the liquid scintillation mixture Ultima Gold™ were purchased from PerkinElmer Life Sciences. [4-^{14}C]3α-Androstanediol and [4-^{14}C]3β-androstanediol were synthesized enzymatically from [4-^{14}C]DHT using recombinant AKR1C9 and recombinant AKR1C1, respectively. All unlabeled steroids were obtained from Steraloids (Wilton, NH). Flufenamic acid was purchased from ICN Biomedical Inc. (Aurora, OH). Deuterated chloroform ($CDCl_3$, 99.9 atom % D) was obtained from Aldrich. Pyridine nucleotides were purchased from Roche Applied Science. TRIzol LS reagent, Superscript II preamplification system and oligonucleotide primers were obtained from Invitrogen. Human tissue RNA was purchased from BD Bioscience Clontech (Palo Alto, CA). All other reagents were of American Chemical Society grade or better.

Expression and Purification of Recombinant Human AKR1C Isoforms—Recombinant human AKR1C isoforms were overexpressed in *Escherichia coli* C41(DE3) host cells transformed with the inducible prokaryotic expression vectors pET-16b as described previously (38, 39). Transformed cells were grown in cultures of LB media containing 100 μg/ml ampicillin, and nontransformed control cells were grown in cultures of LB media without ampicillin. Upon reaching an A_{600} of 0.6, isopropyl-1-thio-β-D-galactopyranoside (1 mM) was added to induce enzyme expression overnight. Bacterial sonicates were prepared and aliquots were centrifuged for 1 h at 100,000 × *g* and 4 °C to obtain cytosolic enzyme preparations.

Recombinant enzymes were purified to homogeneity from the sonicates by sequential chromatography on a DE52 anion exchange and a Sepharose Blue column according to a previously described protocol (38) to yield enzymes of the following specific activities: 0.21 μmol of androsterone (75 μM) oxidized/min/mg (AKR1C4) and 2.1, 2.5, and 2.8 μmol of 1-acenaphthenol (1 mM) oxidized/min/mg (AKR1C1, AKR1C2, and AKR1C3, respectively). Purity of the enzymes was verified by SDS-polyacrylamide gel electrophoresis, and protein concentration was determined (40). The homogeneous enzymes were stored in aliquots at −80 °C.

Radiometric Assays—Standard incubations were conducted in a final volume of 100 μl containing 37.5 μM unlabeled steroid and 3.75 μM (0.02 μCi) amounts of the respective 4-^{14}C-labeled compound in 100 mM potassium phosphate buffer (pH 7.0) with 2.3 mM NADPH and 4% acetonitrile. Reactions were started by the addition of either 1 μl of purified enzyme (5.0, 6.2, 5.8, 9.0, and 7.2 μg of purified AKR1C1, AKR1C2, AKR1C3, AKR1C4, and AKR1C9, respectively) or 1 μl of bacterial cytosol (containing 10.3, 4.7, 6.4, 5.5, and 8.1 μg of cytosolic protein from AKR1C1, AKR1C2, AKR1C3, AKR1C4, and AKR1C9 transformed cells, respectively, or 8.6 μg of cytosolic protein from non-transformed control cells) and incubated at 37 °C. Reactions were ter-

minated by the addition of 500 μl of ice-cold ethyl acetate and steroids extracted by continuous vortexing for 5 min. The organic phases were transferred into a glass tube, and the extraction step was repeated once. The combined organic phases were evaporated to complete dryness.

The dried extracts were redissolved in 40 μl of ethyl acetate and applied to LK6D Silica TLC plates (Whatman Inc., Clifton, NJ). Remaining residues of the extracts were redissolved in 40 μl of chloroform/ethanol (35:15, v/v) containing 25 μg each of nonradioactive reference steroids: androstanedione, DHT, androsterone, 3α-Diol, and 3β-Diol. Epiandrosterone was not used because it could not be separated from androsterone. The chloroform/ethanol mixtures were then applied to the LK6D Silica TLC plates on top of the corresponding first spot. The chromatograms were developed in chloroform/ethyl acetate (4:1, v/v) as follows: (i) the TLC plates were predeveloped three times until the solvent front reached 5, 8, and 12 mm above the origin, and (ii) the plates were fully developed twice. The TLC plates were completely dried between steps. Co-chromatographed reference steroids were stained by spraying with an acetic acid/sulfuric acid/anisaldehyde (100:2:1, v/v/v) solution and heating. The amounts of substrate and products were quantified by scraping the corresponding silica gel sections into scintillation fluid. Radioactivity was counted as automatically quench-corrected dpm with a TriCarb 2100 (Packard Instrument, PerkinElmer Life Sciences). The relative amount of each corresponding radioactive steroid was calculated as percentage of the total radioactivity recovered from a single TLC lane. Blank values were subtracted. For autoradiography analysis the TLC plates were exposed to x-ray film prior to scraping.

Determination of Steady State Kinetic Parameters—The $k_{cat(app)}$ values for DHT reduction catalyzed by the 3α-HSD and 3β-HSD activities of the AKR1C isoforms were calculated using the exact molecular weight of the AKR1C isoforms to convert specific enzyme activities obtained from time courses, which were followed radiometrically. K_M values for the reduction of DHT were previously determined to range from 8.3 ± 1.5 μM (AKR1C4) to 80.6 ± 28.8 μM (AKR1C1) in radiometric assays (34). In the assays performed here, the final substrate concentration was 41.25 μM, which is the solubility limit of DHT in the incubation systems. Because saturation was not achieved for each isoform, k_{cat} values were considered apparent values. Specific enzyme activities were calculated by determination of the tangents to the linear part of the exponential fit of the untransformed progress curve. Nonlinear curve fitting was performed with the Fig.P 2.7 program for Windows (Biosoft, Cambridge, United Kingdom) using the equation for pseudo-first order decay: $[P]_t = [S]_0 (1 - e^{-kt})$.

Enzymatic Synthesis of [4-^{14}C]3α-Diol and [4-^{14}C]3β-Diol Substrates—Two μCi [4-^{14}C]DHT were evaporated to dryness under a gentle stream of nitrogen and redissolved in 40 μl of acetonitrile. The steroid substrate was then added to a 1-ml incubation system containing 100 mM potassium phosphate buffer (pH 7.0) and 2.3 mM NADPH. The reaction was started by the addition of excess recombinant AKR1C9 (specific activity of 1.6 μmol of androsterone (75 μM) oxidized/min/mg) (41) and monitored at 340 nm at 25 °C until the predicted absorbance change in NADPH indicated that the entire substrate had been converted to 3α-Diol. The reaction mixture was extracted five times with 2 ml of ethyl acetate, and the pooled extracts were dried over sodium sulfate and evaporated to complete dryness. The residues were redissolved twice in 200 μl of ethyl acetate, and spotted on a 20 × 20-cm TLC glass plate precoated with a 0.25-mm layer of silica gel. Chromatograms were developed in chloroform/ethyl acetate (4:1, v/v) as described above. [4-^{14}C]3α-Diol was isolated after identification of its position on the TLC plate by autoradiography and by comparison to an authentic reference standard. The steroid was eluted from the silica gel four times with 2 ml of ethyl acetate. The pooled extracts were dried over sodium sulfate, evaporated to complete dryness, and redissolved in acetonitrile to yield a stock solution of 0.375 nmol (0.02 μCi)/μl. Recovery of label in [4-^{14}C]3α-Diol was 77.6%.

The synthesis of [4-^{14}C]3β-Diol was conducted in an identical manner, but excess recombinant AKR1C1 was used as the catalyst and the reaction was conducted for 2 h at 37 °C. A stock solution of 0.375 nmol (0.02 μCi)/μl was obtained. Recovery of label in [4-^{14}C]3β-Diol was 67.3%.

Identification of 3α- and 3β-Diol as Products of AKR1C Reduction of DHT by NMR Analysis—To authenticate the identity of the 3α/3β-Diol products formed by the reduction of DHT via AKR1C enzymes, reactions were performed on a large scale. Metabolites were synthesized in a 100-ml system containing 100 mM potassium phosphate buffer (pH 7.0), 1 mM NADPH, and 100 μM unlabeled DHT. The reaction was started by the addition of 1 ml of bacterial cytosol (10.3 mg of protein) from cells overexpressing AKR1C1 and incubated for 2 h at 37 °C. Steroids were extracted twice with 100 ml of ethyl acetate and a third time with 50 ml of ethyl acetate. The pooled extracts were dried over sodium sulfate and evaporated to complete dryness. The residues were redissolved twice in 500 μl of ethyl acetate, and spotted on two 20 × 20-cm TLC glass plates precoated with a 0.25-mm layer of silica gel. 3α-Diol and 3β-Diol were isolated after development in chloroform/ethyl acetate (4:1, v/v) as described above. The steroid products were eluted from the corresponding silica gel fractions three times with 6 ml of ethyl acetate. The pooled elutes were dried over sodium sulfate, evaporated to complete dryness, and redissolved in 1 ml of $CDCl_3$. The redissolved samples were again evaporated to complete dryness and redissolved in 1 ml of $CDCl_3$.

^{1}H NMR (nuclear magnetic resonance) data were collected on a Varian Unity 500 Spectrometer operating at 500 MHz, using $CDCl_3$ as the solvent. Chemical shifts are reported relative to tetramethylsilane at 0.00 ppm with the residual signal of $CDCl_3$ serving as the secondary reference at 7.24 ppm.

Synthesis of AKR1C1–AKR1C4 Full-length Standard cDNAs—Standard complementary DNA (cDNA) of AKR1C1–AKR1C4 was excised from the prokaryotic expression vectors pET-16b containing the respective cDNA clones (38) via digestion with XhoI and BglII. Digestion products were size-fractionated on a 1% agarose gel, and the respective cDNA bands were purified from the gel with the QIAquick gel extraction kit (Qiagen Inc., Valencia, CA). The procedure yielded full-length double-stranded cDNA of the isoforms with an additional 105-bp vector DNA at the 5′ end of the leading strand.

RT-PCR Analyses—Total RNA was extracted from HepG2 cells using the TRIzol reagent. Reverse transcription (RT) of 1 μg of total RNA with Superscript II reverse transcriptase was performed according to the protocol from the manufacturer. RT was performed at 42 °C for 50 min and was terminated by denaturing the reverse transcriptase at 70 °C for 15 min.

Polymerase chain reactions (PCRs) were conducted using 100 ng of HepG2 cDNA and human tissue cDNA samples, respectively. In a final volume of 50 μl the PCR systems contained 2.5 units of *Taq* DNA polymerase (Promega Corp., Madison, WI), 2.5 mM $MgCl_2$, 0.2 mM each dNTP, and 20 pmol of the respective oligonucleotide primers. In addition, the PCR systems for the amplification of AKR1C2, AKR1C4, and β-actin transcripts contained 2.5 μl of dimethyl sulfoxide. To amplify the transcripts of the AKR1C isoforms, the β-actin housekeeping gene and the 3β-HSD/KSI isoforms, oligonucleotide primers crossing intron-exon boundaries were used as described (34, 42). PCR was initiated by a 5-min denaturation step at 94 °C. The isoform-specific oligonucleotide primers utilized for amplification of AKR1C1–AKR1C4 transcripts yielded PCR products of the same size of 590 bp. The PCR program for amplification of the AKR1C transcripts consisted of 30 cycles with a 45-s denaturation step at 94 °C, followed by a 45-s annealing step (at 55 °C for AKR1C4, 60 °C for AKR1C1 and AKR1C3, or 62 °C for AKR1C2) and a 2-min extension step at 72 °C. The pair of oligonucleotide primers used for amplification of the β-actin transcript yielded a 838-bp PCR product. The respective PCR program consisted of 30 cycles with a 30-s denaturation step at 94 °C, followed by a 60-s annealing step at 60 °C and a 2-min extension step at 72 °C. The pair of oligonucleotide primers utilized for amplification of the highly homologous 3β-HSD/KSI transcripts detected both known human isozymes and gave the same amplified cDNA size of 790 bp in RT-PCR. The respective PCR program consisted of 35 cycles with a 45-s denaturation step at 94 °C, followed by a 45-s annealing step at 64 °C and a 2-min extension step at 72 °C. A 10-min final extension step at 72 °C completed all PCR protocols. The products were resolved on 2% agarose gels containing ethidium bromide and then visualized under ultraviolet light using the digital GDS-8000 UVP BioImaging System (UVP, Inc., Upland, CA).

Optical Density Analysis—Optical density analyses were carried out to determine the amount of AKR1C1–AKR1C4 products amplified from total HepG2 cDNA in comparison to the amount of PCR products amplified from 25, 2.5, or 0.25 ng of the respective authentic full-length standard cDNAs. PCR products were size-fractionated on 2% agarose gels and evaluated with the digital GDS-8000 UVP imaging system. Densitometric analysis of the appropriate bands and the background was performed using the Labworks™ software (UVP, Inc.). Linear regression analyses of the data (with the concentration of standard cDNA in the log scale) gave the approximate mRNA concentration in HepG2 cells.

Cell Culture Experiments—HepG2 cells were obtained from the American Type Culture Collection (ATCC, Manassas, VA). Cells (4×10^6) were maintained in 60-mm dishes at 37 °C and 5% CO_2 containing 5 ml of Dulbecco's modified Eagle's medium supplemented with 500 units of penicillin, 500 units of streptomycin, 2 mM L-glutamine, and

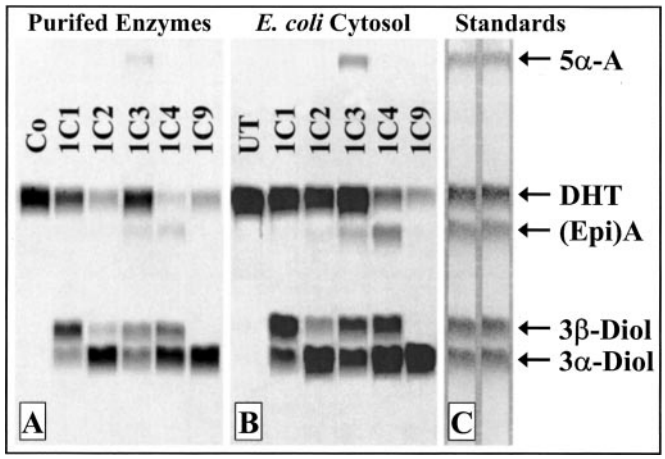

FIG. 2. **Human AKR1C isoforms reduce 3-ketosteroids into 3α- and 3β-hydroxysteroids.** Autoradiograms of TLC analyses of the NADPH-dependent reduction of [4-^{14}C] DHT are shown. *Panel A*, incubations of a no-enzyme control (*Co*), 90 min; homogeneous recombinant AKR1C1, 30 min; AKR1C2, 30 min; AKR1C3, 90 min; AKR1C4, 30 min, and AKR1C9, 5 min. *Panel B*, incubations of cytosolic preparations from (*UT*) untransformed *E. coli* host cells, 90 min, or from host cells transformed to overexpress AKR1C1, 30 min; AKR1C2, 30 min; AKR1C3, 90 min; AKR1C4, 30 min, and AKR1C9, 5 min. *Panel C* shows a photograph of co-chromatographed and stained nonradioactive standards: androstanedione (*5α-A*), DHT, (epi)androsterone (*Epi(A)*), 3β-Diol, and 3α-Diol. Assays were performed as described under "Experimental Procedures," and chromatograms were exposed to x-ray film at −70 °C for 24 h.

10% fetal bovine serum. To measure DHT metabolism, cells were incubated in 5 ml of fresh medium containing 10 μM DHT (including 0.4 μCi [4-^{14}C]DHT). In the inhibition experiments, an additional 100 μM flufenamic acid was added. Aliquots (150 μl) of the medium were withdrawn twice from each dish at 0, 1, 3, 6, and 9 h, diluted with 350 μl of ice-cold H_2O, and extracted twice with 2 ml of water-saturated ice-cold ethyl acetate. The extracts were dried. Redissolved extracts and nonradioactive reference steroids were applied to LK6D Silica TLC plates as described above. In this instance, chromatograms were developed three times in dichloromethane/diethyl ether (11:1, v/v) to gain complete separation of the reference standards. All cell incubations were performed in triplicate.

Molecular Docking Simulations—Simulations of DHT binding in the active sites of AKR1C1 and AKR1C2 were performed using the AutoDock program (version 3.0) (43). Protein Data Bank (PDB) entries 1MRQ (37) and 1IHI (35) were used as the starting structures for the docking of the steroid into AKR1C1 and AKR1C2, respectively. Existing solvent molecules and steroid ligands were removed to generate docking targets containing one molecule of the respective enzyme and the $NADP^+$ cofactor. Because the reaction of interest was the reduction of DHT, docking calculations were also performed using targets containing the reduced cofactor NADPH with either a planar (PDB entry 1AOE) or a bent nicotinamide ring (PDB entry 1HET) overlaid onto the $NADP^+$ position. The coordinates of DHT were taken from the PDB entry 1D2S. The starting position of DHT for docking simulations was >40 Å away from the center of the steroid binding cavities. Docking computations were performed using the Lamarckian genetic algorithm and simulated annealing protocols. Each protocol consisted of 50–200 runs, with each run producing a docked conformer. Cluster analysis was performed, which grouped the conformers with root mean square deviation in atomic positions of less than 1.0 Å into one cluster and ranked clusters by docking energy.

RESULTS

Reassessment of DHT Reduction Catalyzed by Human AKR1C Isoforms—We have previously shown that human AKR1C1–AKR1C4 are non-positional-specific HSDs and display 3α-, 17β-, and 20α-HSD activities in varying ratios (34). To further address the substrate specificities of these isoforms, we developed an improved TLC system, which permitted the separation of authentic DHT, androstanedione, (epi)androsterone, 3α-Diol, and 3β-Diol (Fig. 2*C*). Using this method, we observed that purified homogeneous recombinant AKR1C1–AKR1C4 generated two major products from the NADPH-dependent reduction of DHT. One product co-migrated with an authentic 3α-Diol standard and the other with an authentic 3β-Diol standard (Fig. 2*A*). In contrast to the human AKR1C isoforms, recombinant rat liver AKR1C9 generated only one product, co-migrating with the 3α-Diol standard. To validate that the recombinant human proteins were responsible for the 3α- as well as the 3β-reaction and that the latter reaction was not the result of contaminating 3β-HSD from the *E. coli* host cells, we showed that cytosolic preparations from untransformed *E. coli* host cells were incapable of catalyzing the reduction of DHT (Fig. 2*B*). By contrast, cytosolic preparations from *E. coli* host cells transformed to overexpress the recombinant AKR1C isoforms showed time-dependent formation of 3α-Diol and 3β-Diol characteristic of the homogeneous recombinant AKR1C isoforms (Figs. 2*B* and 3).

Structure Identity of 3α- and 3β-Diol Produced by AKR1C Activity—Further validation of the 3α/3β-HSD activities of the AKR1C isoforms involved ^{1}H NMR structural verification that the products of the AKR1C reactions were 3α- and 3β-Diol. The products were enzymatically prepared from 2.9 mg of DHT as described under "Experimental Procedures" using adequate amounts of a cytosolic preparation from *E. coli* host cells transformed with AKR1C1. AKR1C1 was used as the enzyme source because of its relatively high 3β-HSD activity and the fact that it generated reasonable amounts of both 3α- and 3β-Diol without catalyzing the formation of additional DHT metabolites (Figs. 2 and 3). Two DHT metabolites were isolated, a minor product of ~0.5 mg and a major product of ~1.8 mg. The ^{1}H NMR spectrum of the minor product exhibited the characteristic spectrum of an authentic 3α-Diol standard (δ 0.71 (s, 3H, CH_3, C18), δ 0.77 (s, 3H, CH_3, C19), δ 3.61 (t, 1H, 17α, J = 8.5), δ 4.02 (m, 1H, 3β)). This spectrum showed separate resonances for the 17α proton, which was present as a triplet, and the 3β-equatorial proton, which was present as a downfield collapsed multiplet (Fig. 4, *A* and *B*). By contrast, the ^{1}H NMR spectrum of the major product resembled the characteristic spectrum of an authentic 3β-Diol standard (δ 0.71 (s, 3H, CH_3, C18), δ 0.81 (s, 3H, CH_3, C19), δ 3.59–3.62 (m, 3α- and 17α-protons)). The multiplet for the 3α-axial proton is upfield and superimposed upon the triplet for the 17α proton (Fig. 4, *C* and *D*), which is characteristic of the 3α-axial proton.

Evidence That 3α- and 3β-Diol Formation Occurs at the Same Active Sites of the Human AKR1C Isoforms—To substantiate that 3α- and 3β-Diol formation occur at the same active site, we exploited our previous observation that AKR1C isoforms are potently and competitively inhibited by NSAIDs (44). Therefore, the effects of increasing flufenamic acid concentrations on DHT reduction catalyzed by the various recombinant isoforms was investigated. Formation of both 3α-Diol and of 3β-Diol were equally sensitive to inhibition by the NSAID (Fig. 5). The corresponding IC_{50} values for the formation of 3α- and 3β-Diol were 9.2 and 10.9 μM for AKR1C1, 5.3 and 14.3 μM for AKR1C2, 6.9 and 7.9 μM for AKR1C3, and 117.3 and 59.2 μM for AKR1C4, respectively. These results are consistent with the two reactions occurring at the same active site of each of the AKR1C isoforms.

Isoform-specific Differences in DHT Reduction Catalyzed by Human AKR1C Isoforms—We observed notable differences in the time courses of 3α- and 3β-Diol formation catalyzed by the various AKR1C isoforms (Fig. 3). AKR1C1 predominantly catalyzed the formation of 3β-Diol, whereas AKR1C2 and AKR1C4 predominantly catalyzed the formation of 3α-Diol. Conversion of 3α-Diol into 3β-Diol was observed with AKR1C4, once the reduction of DHT was complete. Purified AKR1C3

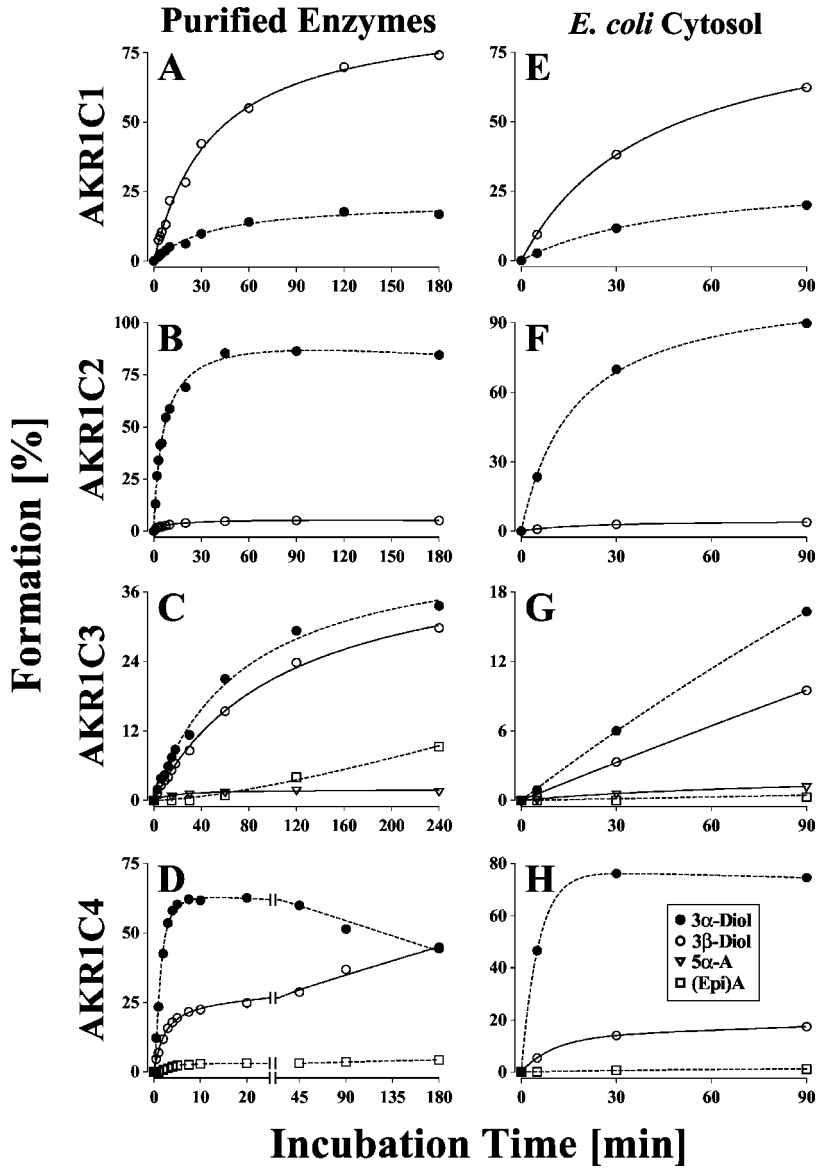

FIG. 3. **Time courses of the NADPH-dependent reduction of DHT into 3α-Diol and 3β-Diol catalyzed by human AKR1C isoforms.** Conversion of DHT into androstanedione (▽), (epi)androsterone (□), 3β-Diol (○), and 3α-Diol (●) by homogeneous recombinant AKR1C1 (*A*), AKR1C2 (*B*), AKR1C3 (*C*), and AKR1C4 (*D*) or by cytosolic preparations of *E. coli* host cells transformed to overexpress AKR1C1 (*E*), AKR1C2 (*F*), AKR1C3 (*G*), and AKR1C4 (*H*). The results represent mean values of assays performed in duplicate as described under "Experimental Procedures."

showed relatively low reductive activity toward DHT, in which the enzyme formed 3α- and 3β-Diol in almost equal amounts. The formation of trace amounts of androstanedione by AKR1C3 and of (epi)androsterone by AKR1C3 and AKR1C4 was also observed. This indicates (i) that DHT is also oxidized to androstanedione via 17β-HSD activity of AKR1C3 using enzyme-generated $NADP^+$ and (ii) that once AKR1C3 and AKR1C4 have reduced DHT to 3α- and 3β-Diol, the products can be oxidized to (epi)androsterone via 17β-HSD activity of the enzymes using enzyme-generated $NADP^+$ (see Fig. 1).

We now report $k_{cat(app)}$ values and specific activities of the turnover of DHT by reductive 3α- and 3β-HSD activity of the AKR1C isoforms (Table I). It is apparent from these values that AKR1C1 has a higher $k_{cat(app)}$ values for the formation of 3β-Diol than for the formation of 3α-Diol. The reverse is true for AKR1C2. Highest $k_{cat(app)}$ values for the formation of 3α-Diol and 3β-Diol were observed with AKR1C4, whereas lowest $k_{cat(app)}$ values were found with AKR1C3.

In conducting these studies, we found that we previously underestimated the kinetic constants for AKR1C2 (34). Therefore, the k_{cat}, K_M, and k_{cat}/K_M values for this enzyme were reassessed radiometrically as well as spectrophotometrically by determination of the initial velocities at varying DHT concentrations from 1.6 to 41.25 μM, yielding k_{cat} and K_M values and their standard errors of mean (45). Spectrophotometric analyses were performed as described (34) by monitoring the decrease in NADPH absorbance at 340 nm except they were conducted at 37 °C. The k_{cat} values obtained by these radiometric analyses were 2.97 ± 0.16 min^{-1} for the formation of 3α-Diol and 0.18 ± 0.01 min^{-1} for the formation of 3β-Diol. The K_M values were 6.6 ± 1.1 μM for the formation of 3α-Diol and 11.0 ± 2.1 μM for the formation of 3β-Diol, resulting in k_{cat}/K_M values of 458 and 19 min^{-1} mM^{-1}, respectively. In comparison, the spectrophotometrically obtained k_{cat} value (no distinction between the formation of 3α- and 3β-Diol) was 3.10 ± 0.30 min^{-1} and the K_M value was 4.3 ± 1.2 μM resulting in a k_{cat}/K_M value of 714 min^{-1} mM^{-1}.

Human AKR1C Isoforms Display Significant 3α[17β]-Hydroxysteroid Oxidase Activity with 3α-Diol as the Substrate—Using enzymatically prepared [4-^{14}C]3α-Diol and [4-^{14}C]3β-Diol as substrates, we determined whether AKR1C1–AKR1C4 displayed 3α- and 3β-hydroxysteroid oxidase activity. Substantial oxidative enzyme activity was observed for AKR1C2, AKR1C3, and AKR1C4 with 3α-Diol as the substrate (Fig. 6*A*), whereas only negligible activity was determined with 3β-Diol (Fig. 6*B*). AKR1C1 demonstrated only very low oxidative catalytic activity toward either substrate, despite its ability to form 3β-Diol from DHT. Furthermore, the experiments showed that

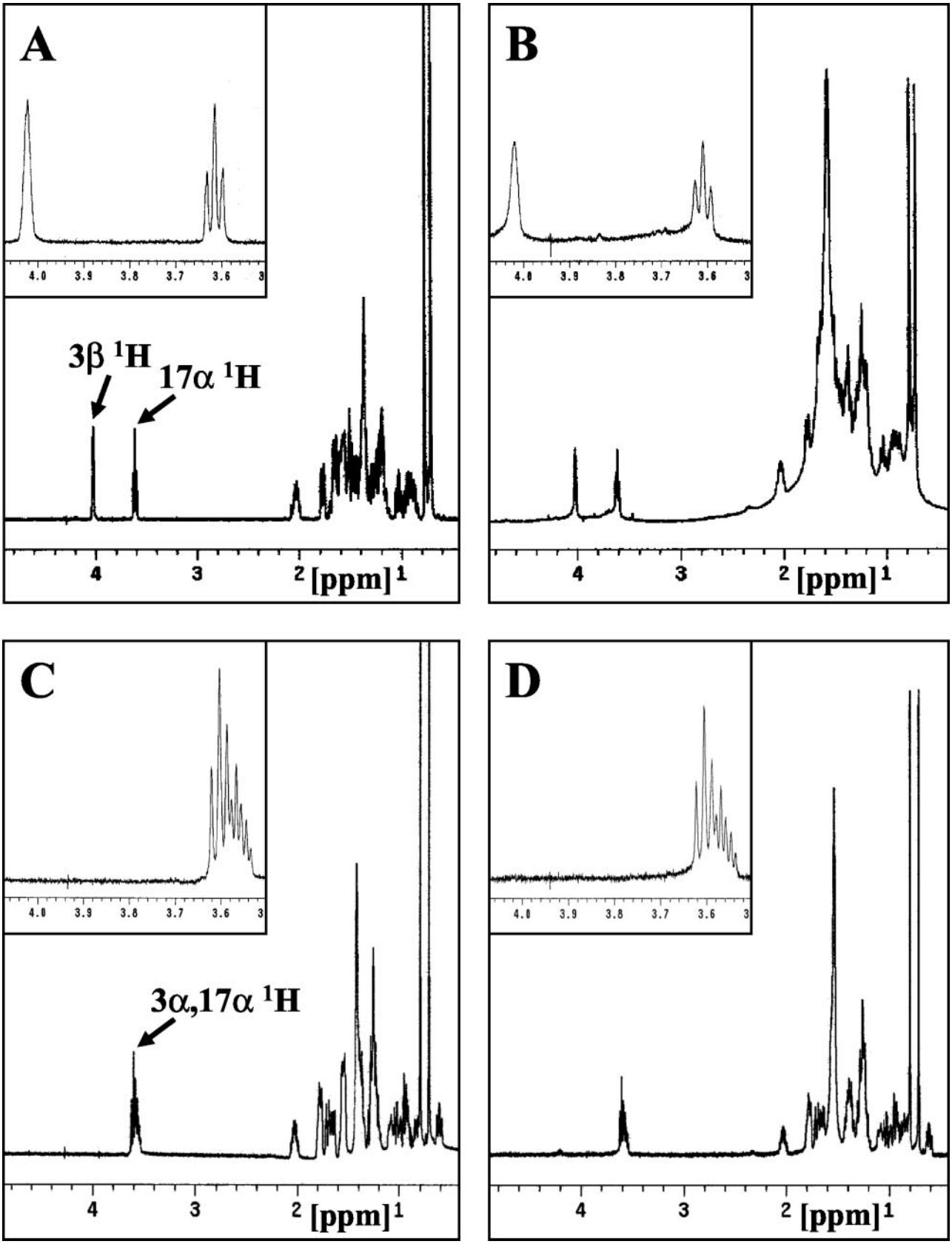

FIG. 4. **^{1}H NMR spectra of 3α- and 3β-Diol.** *A* and *C* are the spectra of authentic 3α- and 3β-Diol standards, respectively. *B* and *D* are spectra of 3α- and 3β-Diol obtained from the reduction of DHT catalyzed recombinant AKR1C1 activity as described under "Experimental Procedures." The *insets* show the expanded regions for the 3α-axial and the 3β-equatorial protons.

in vitro AKR1C2 and AKR1C4 acted as 3α-hydroxysteroid oxidases catalyzing the conversion of 3α-Diol to DHT. In contrast, AKR1C3 predominantly acts as 17β-hydroxysteroid oxidase catalyzing the conversion of 3α-Diol to androsterone. AKR1C2 and AKR1C4 also catalyzed the formation of trace amounts of (epi)androsterone from (3β)3α-Diol, whereas AKR1C3 also cat-

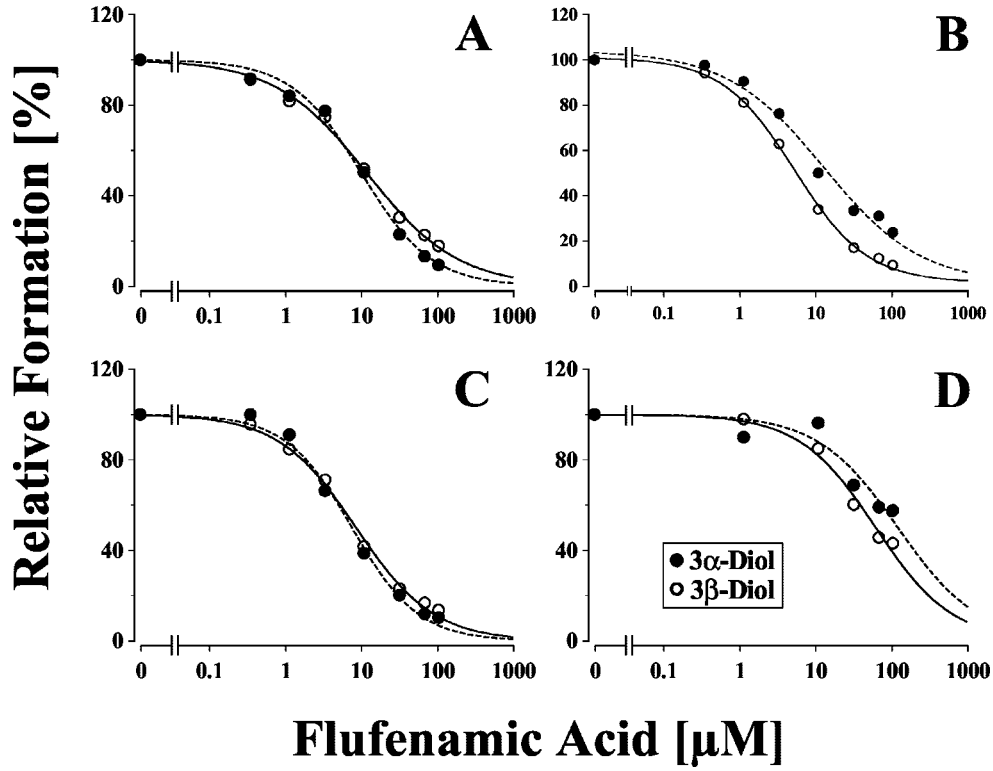

FIG. 5. **The NSAID flufenamic acid shows parallel inhibition of the 3α-/3β-HSD activities of human AKR1C isoforms.** Figure shows NADPH-dependent reduction of DHT into 3β-Diol and 3α-Diol catalyzed by homogeneous recombinant AKR1C1 (*A*), AKR1C2 (*B*), AKR1C3 (*C*), and AKR1C4 (*D*). Incubations were conducted for 1 min (AKR1C4), 4 min (AKR1C2), 20 min (AKR1C1), or 60 min (AKR1C3) with increasing inhibitor concentrations. The results represent mean values of assays performed in duplicate as described under "Experimental Procedures."

TABLE I
NADPH-dependent reduction of DHT to 3α-Diol and 3β-Diol by homogeneous recombinant human AKR1C1-AKR1C4 isoforms

Products	1C1		1C2		1C3		1C4	
	Specific activity[a]	$k_{cat(app)}$	Specific activity	$k_{cat(app)}$	Specific activity	$k_{cat(app)}$	Specific activity	$k_{cat(app)}$
	nmol min^{-1} mg^{-1}	*min^{-1}*	*nmol min^{-1} mg^{-1}*	*min^{-1}*	*nmol min^{-1} mg^{-1}*	*min^{-1}*	*nmol min^{-1} mg^{-1}*	*min^{-1}*
3α-Diol	3.9	0.15	**76.1**	**2.81**	**3.7**	**0.14**	**119.1**	**4.41**
3β-Diol	**16.1**	**0.60**	3.8	0.14	2.5	0.09	32.8	1.22
Ratio 3α/3β	0.25		20.07		1.55		3.61	

[a] Specific activities (nmol min^{-1} mg^{-1}), $k_{cat(app)}$ values (min^{-1}), and ratio of 3α-Diol *versus* 3β-Diol formation (ratio 3α/3β) were obtained from time-course analyses as described under "Experimental Procedures."

alyzed the formation of trace amounts of DHT from the Diols. This demonstrates that AKR1C2 and AKR1C4 display low 17β-hydroxysteroid oxidase activity in addition to their 3-hydroxysteroid oxidase activity and that AKR1C3 displays low 3-hydroxysteroid oxidase activity in addition to its predominant 17β-hydroxysteroid oxidase activity. Consequently, combined 3-hydroxysteroid oxidase and 17β-hydroxysteroid oxidase activity of the isoforms resulted in the formation of some androstanedione from the Diols (Fig. 6, and see Fig. 1). Interestingly, formation of 3β-Diol was also observed when AKR1C4 was incubated with 3α-Diol, suggesting that, *in vitro*, epimerization can occur via the DHT intermediate. A summary of the specific activities for 3α/3β-Diol oxidation catalyzed by the AKR1C isoforms is given in Table II. The estimated specific activities of the oxidative reactions (Table II) were not transformed into $k_{cat(app)}$ values, because the K_M values for these reactions with saturating NAD^+ as the cofactor could not be estimated.

Influence of the NADPH/NAD$^+$ Ratio on the Oxidoreductase Activities of AKR1C Isoforms—A previous study demonstrated that, *in vitro*, the NAD^+-dependent 3α-hydroxysteroid oxidase of AKR1C2 was potently inhibited by low micromolar NADPH concentrations, whereas its NADPH-dependent 3-ketosteroid reductase activity was not inhibited by the opposing cofactor NAD^+ (46). To determine whether the other AKR1C isoforms have similar properties, we investigated the influence of the NADPH/NAD^+ ratio on (i) their *in vitro* 3-ketosteroid reductase activity using DHT as the substrate and (ii) their *in vitro* 3α[17β]-hydroxysteroid oxidase activity using 3α-Diol as the substrate. NADPH-dependent 3-ketosteroid reductase activity of the enzymes was not inhibited by NAD^+, although in the inhibition experiment equal concentrations of the two cofactors were present (Fig. 7*A*; 1 mM NADPH plus 1 mM NAD^+ final concentrations). On the other hand, NAD^+-dependent hydroxysteroid oxidase activity of the isoforms was potently inhibited by low micromolar concentrations of NADPH (Fig. 7*B*; 0.01 mM NADPH plus 1 mM NAD^+ final concentrations).

Expression of AKR1C1–AKR1C4 and 3β-HSD/KSI in HepG2 Cells—To determine the contribution of AKR1C isoforms on the reduction of DHT *in vivo*, we investigated their mRNA expression levels *versus* 3β-HSD/KSI in the human HepG2 cell line. Using authentic full-length standard cDNA of AKR1C1–AKR1C4 as controls, we adjusted PCR conditions to achieve isoform specificity over 30 cycles (data not shown). Utilizing isoform-specific PCR methods reasonable mRNA expression of AKR1C1–AKR1C3 in HepG2 cells could be confirmed, whereas limited expression of AKR1C4 was found (Fig. 8, *A* and *B*). Optical density analyses of the PCR products from 25, 2.5, or

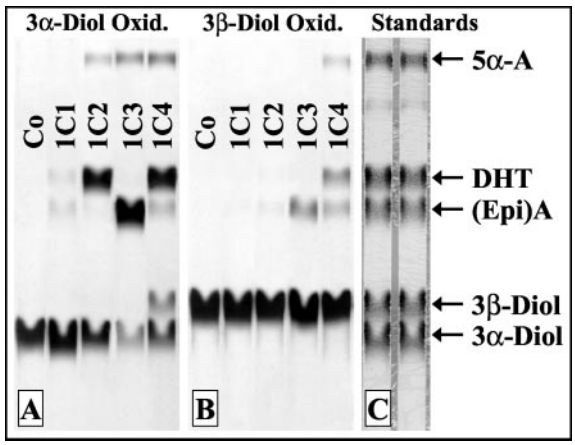

FIG. 6. **Human AKR1C isoforms oxidize 3α- and 3β-hydroxysteroids.** Autoradiograms of TLC analyses are shown. *Panel A*, the NAD^+-dependent oxidation of [4-^{14}C]3α-Diol; *panel B*, the NAD^+-dependent oxidation of [4-^{14}C]3β-Diol. Incubations were as follows: no enzyme controls (*Co*), 120 min; homogeneous recombinant AKR1C1, 120 min; AKR1C2, 120 min; AKR1C3, 120 min; and AKR1C4, 60 min. *Panel C* shows a photography of co-chromatographed and stained non-radioactive standards: androstanedione (*5α-A*), DHT, (epi)androsterone (*Epi(A)*), 3β-Diol and 3α-Diol. Assays were performed as described under "Experimental Procedures," and chromatograms were exposed to x-ray film at −70 °C for 24 h.

0.25 ng of full-length standard cDNAs were performed to yield standard curves. Those standard curves enabled the direct quantification of AKR1C1–AKR1C3 mRNA expression in total RNA extracts of HepG2 cells; AKR1C1 showed an expression of 4.9 ng, AKR1C2 of 0.46 ng, and AKR1C3 of 0.75 ng per μg of total RNA.

Investigation of the mRNA expression of the two human 3β-HSD/KSI isoforms in HepG2 cells in comparison to a variety of human tissues revealed no significant expression of either isoform in HepG2 cells (Fig. 8*C*). This was the case although 35 cycles of PCR were performed in contrast to the 30 cycles for the amplification of the AKR1C isoforms.

Inhibition of the Time-dependent Reduction of DHT in HepG2 Cells by Flufenamic Acid—The fact that the human HepG2 cell line expresses significant amounts of AKR1C1–AKR1C3 mRNA but expresses neither 3β-HSD/KSI isoform provides an optimal model to study the impact of the AKR1C isoforms on the *in vivo* metabolism of DHT. Time-dependent metabolism of DHT (10 μM final concentrations) in HepG2 cell culture produced three major metabolites: 3α-Diol, 3β-Diol, and (epi)androsterone (Fig. 9, *A* and *C*). The formation of 3α-Diol and 3β-Diol reflects the direct impact of 3-ketosteroid reductase activity of the AKR1C isoforms. The formation of (epi)androsterone reflects the combined effects of the 3-ketosteroid reductase activity of the AKR1C isoforms plus the oxidative activity of (an)other 17β-HSD(s) (see Fig. 1). The role of AKR1C isoforms in DHT metabolism in HepG2 cells was verified by determining the inhibitory effects of flufenamic acid (100 μM final concentration). A significant reduction of the formation of the three metabolites was observed when flufenamic acid was present (Fig. 9, *B* and *D*). After 9 h, the formation of 3α-Diol was reduced by 74.2%, the formation of 3β-Diol by 57.5%, and the formation of (epi)androsterone by 50.4%. In contrast, in the presence of flufenamic acid, the formation of androstanedione from DHT via endogenous oxidative 17β-HSD activity (see Fig. 1) was increased by 688%. This was the result of diminished 3-ketosteroid reductase activity of the AKR1C isozymes, which results in higher DHT concentrations for the other 17β-HSD(s).

Molecular Docking Simulations of the Preferred Position of DHT in the Active Sites of AKR1C1 and AKR1C2—To determine whether we could rationalize why AKR1C1 was predominantly a 3β-HSD and AKR1C2 was a 3α-HSD, we exploited the available crystal structures of these enzymes to perform molecular docking simulations. To validate the docking method, the positions of 20α-hydroxyprogesterone in the AKR1C1-$NADP^+$-20α-hydroxyprogesterone and ursodeoxycholate in the AKR1C2-$NADP^+$-ursodeoxycholate ternary complexes were reproduced by docking the steroid molecules into the targets containing the respective enzyme and $NADP^+$ (starting positions >20 Å away). The root mean square deviations between the docked conformers and the position of the steroids in the crystal structures were 0.8 Å in AKR1C1 and 0.7 Å in AKR1C2. Docking simulations of DHT binding using targets containing three different cofactors ($NADP^+$, and planar or bent NADPH) produced similar clusters of docked conformers. This strongly suggests that the amino acid residues lining the steroid binding site exert a more important role in determining the binding orientation of the substrate than the oxidation state of the cofactor. The preferred docking orientation of DHT differed in the AKR1C1 and the AKR1C2 target structures (Fig. 10). With AKR1C1, the conformers in the cluster with the lowest energy (found 83 times in 200 runs) represent a DHT binding mode that explains the formation of 3β-Diol. The C3-ketone of DHT is in close proximity to the C4 of nicotinamide (3.8 Å) and the α-face of the steroid is directed to the 4-*pro*-R hydrogen. In contrast, a predominate DHT binding mode observed in AKR1C2 (94 times in 200 runs) depicts the positional arrangement between DHT and NADPH for the formation of 3α-diol. The C3-ketone group is 3.6 Å away from the C4 of nicotinamide and the β-face of the steroid is directed to the 4-*pro*-R hydrogen. In summary, in AKR1C1 the A-ring of the steroid has swung relative to its position in AKR1C2 to permit inversion of the stereochemistry of hydride transfer.

DISCUSSION

To date, no enzyme has been assigned to account for the observed NADPH-dependent cytosolic formation of 3β-tetrahydrosteroids. This reaction, which occurs in human androgen target and nontarget tissues, is of significance for the inactivation of DHT to 3β-Diol (3, 5, 6, 8, 9). Human AKR1C1–AKR1C4 isoforms are known to act as non-positional-specific 3α-/17β-/20α-HSDs (34). We have now investigated whether these cytosolic HSDs would also act in a non-stereo-selective manner. Historically, HSDs were considered to catalyze the interconversion of ketone and hydroxyl groups on steroid hormones in a positional and stereo-specific manner (47). Our study shows that the human AKR1C isoforms appear to violate both assumptions. We revealed that AKR1C isoforms reduce DHT into both 3α- and 3β-Diol and demonstrated the *in vivo* significance of this observations in HepG2 cells. Molecular docking simulations rationalized the differences in stereochemical preferences of AKR1C1 and AKR1C2.

3β-HSD activity of recombinant AKR1C isoforms is not the result of residual or contaminating bacterial proteins that co-purified with the human enzymes from the *E. coli* host. Cytosol from untransformed cells was incapable of catalyzing the reduction of DHT (Fig. 2*B*), whereas cytosol from transformed host cells gave the same product profiles as the respective homogeneous recombinant enzymes (Fig. 3). The identity of 3α- and 3β-Diol produced by the AKR1C isoforms was substantiated by ^{1}H NMR spectroscopy because their spectra were identical to authentic standards (Fig. 4). The NSAID flufenamic acid (a known competitive inhibitor of AKR1C enzymes) (44) inhibited 3-ketosteroid reductase activity of all human isoforms in a concentration-dependent manner (Fig. 5). Similar IC_{50} values for the inhibition of reductive 3α- and 3β-HSD activity were observed, which is consistent with the two reactions oc-

TABLE II
Products of NAD$^+$ dependent oxidation of 3α-Diol and 3β-Diol by homogeneous recombinant human AKR1C1-AKR1C4 isoforms

Products	3α-Diol oxidation[a]				3β-Diol oxidation			
	1C1	1C2	1C3	1C4	1C1	1C2	1C3	1C4
	nmol min^{-1} mg^{-1}				*nmol min^{-1} mg^{-1}*			
DHT	0.1	**10.7**	0.4	**234.0**				0.6
(Epi)A	0.1	0.9	**23.0**	0.8		0.1	0.3	0.3
5α-A		0.2	0.3	1.4				0.1
3β-Diol				2.7				

[a] Specific activities for the formation of DHT, (epi)androsterone ((Epi)A), androstanedione (5α-A), and 3β-Diol were obtained from time-course analyses as described under "Experimental Procedures."

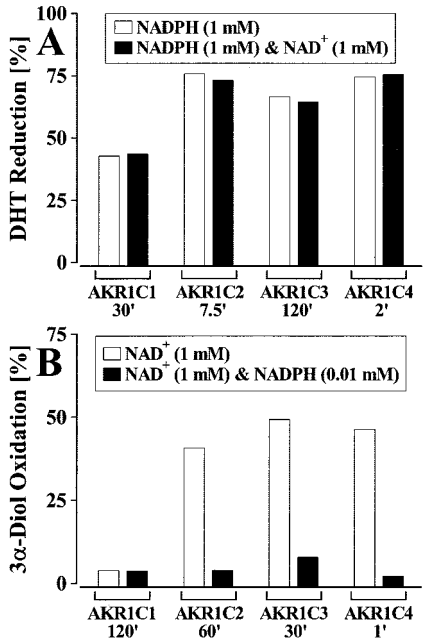

FIG. 7. **NADPH is a potent inhibitor of the NAD$^+$-dependent oxidation of 3α-Diol catalyzed by homogeneous recombinant human AKR1C isoforms.** *Panel A*, inhibitory effects of NAD$^+$ on the NADPH-dependent reduction of DHT were investigated using either 1 mM NADPH alone (*open bars*) or 1 mM NADPH and 1 mM NAD$^+$ in combination (*solid bars*); incubations were conducted for 2 min (AKR1C4), 120 min (AKR1C3), 7.5 min (AKR1C2), or 30 min (AKR1C1). *Panel B*, inhibitory effects of NADPH on the NAD$^+$-dependent oxidation of 3α-Diol were investigated using either NAD$^+$ alone (*open bars*) or 1 mM NAD$^+$ and 0.01 mM NADPH in combination (*solid bars*); incubations were conducted for 1 min (AKR1C4), 30 min (AKR1C3), 60 min (AKR1C2), or 120 min (AKR1C1). The results represent mean values of incubations performed in duplicate as described under "Experimental Procedures."

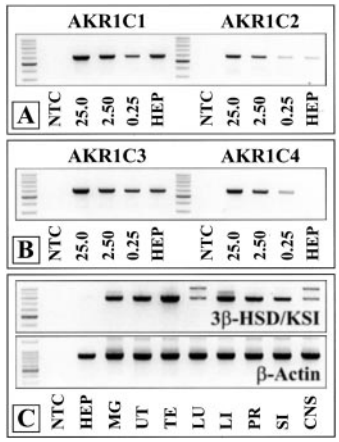

FIG. 8. **AKR1C1–AKR1C4 and 3β-HSD/KSI mRNA expression in HepG2 cells.** *Panels A* and *B*, isoform-specific RT-PCR analyses (30 cycles) of AKR1C1–AKR1C4 expression in total RNA (1 μg) of HepG2 cells (*HEP*) in comparison to the amplification of full-length standard cDNAs (25, 2.5, and 0.25 ng) as positive controls and no template negative controls (*NTC*); *panel C*, RT-PCR analyses of the expression of 3β-HSD/KSI (35 cycles) and the β-actin housekeeping gene (30 cycles) in total RNA (1 μg) from HepG2 cells (*HEP*) and human tissues: *MG*, mammary gland; *UT*, uterus; *TE*, testis; *LU*, lung; *LI*, liver; *PR*, prostate; *SI*, small intestine; *CNS*, central nervous system. The intensified band in the 100-bp ladder as DNA size marker indicates the position of the 500-bp DNA fragment.

curring at the same active site of the AKR1C isoforms.

Time-course analyses of DHT reduction (Fig. 3) revealed distinct catalytic properties of the highly homologous isoforms, which were evident in $k_{cat(app)}$ values for the formation of 3α- and 3β-Diol (Table I). Consequently, the ratios of reductive 3α-HSD *versus* reductive 3β-HSD activity varied significantly among the isoforms in such a manner that AKR1C1 has to be considered a 3β-HSD with subsidiary 3α-HSD activity, AKR1C2 is a strong almost exclusive 3α-HSD, AKR1C3 is a weak dual active 3α- and 3β-HSD, and AKR1C4 is a strong 3α-HSD with subsidiary 3β-HSD activity.

It is apparent that previously published kinetic steady-state constants of the AKR1C isoforms for the reduction of DHT (34) were assigned to a combination of 3α-HSD and 3β-HSD activities. To compare those previous values with the present data, the $k_{cat(app)}$ values for the formation of 3α- and 3β-Diol (Table I) were combined. These total $k_{cat(app)}$ values resembled the previously determined k_{cat} values (0.75 *versus* 0.66 min^{-1} for AKR1C1, 0.23 *versus* 0.25 min^{-1} for AKR1C3 and 5.63 *versus* 1.92 min^{-1} for AKR1C4) (34). However, the estimated total $k_{cat(app)}$ value of AKR1C2 was more than 1 order of magnitude higher than the previously determined k_{cat} value (2.95 *versus* 0.23 min^{-1}) (34). Thus, we previously underestimated the kinetic constants for the reduction of DHT by AKR1C2. Therefore, the kinetic constants for this reaction were redetermined, and the results demonstrated that, when acting as 3-ketosteroid reductase, AKR1C2 is almost as efficient as AKR1C4 (34).

A gradual epimerization of 3α-Diol into 3β-Diol via the DHT intermediate was observed when investigating AKR1C4 activity *in vitro*. This was observed when the reduction of DHT (Fig. 3*D*) or the oxidation of 3α-Diol (Fig. 6*A*) was studied. The observations reflect the enzymatic cycling of products. During the reduction of DHT enzymatically produced NADP$^+$ can oxidize 3α-Diol to yield DHT via 3α-hydroxysteroid oxidase activity of AKR1C4. During the oxidation of 3α-Diol, enzymatically produced NADH can reduce DHT via 3-ketosteroid reductase activity to yield 3α- and 3β-Diol. Consequently, the lack of substantial 3β-hydroxysteroid oxidase activity in AKR1C4 leads to a slow epimerization of 3α-Diol into 3β-Diol over time. This *in vitro* phenomenon is equivalent to the one previously described for NAD(H)-dependent RoDH-like 3α-HSD (32, 48).

Examination of the oxidative activity of the isoforms showed that AKR1C1 is a poor 3-hydroxysteroid oxidase (Fig. 6; Table II), indicating that the enzyme is not bidirectional even *in vitro*. AKR1C3 mainly acted as an efficient 17β-hydroxysteroid oxidase, whereas AKR1C2 and AKR1C4 mainly acted as 3α-hydroxysteroid oxidases. These data support previous findings on

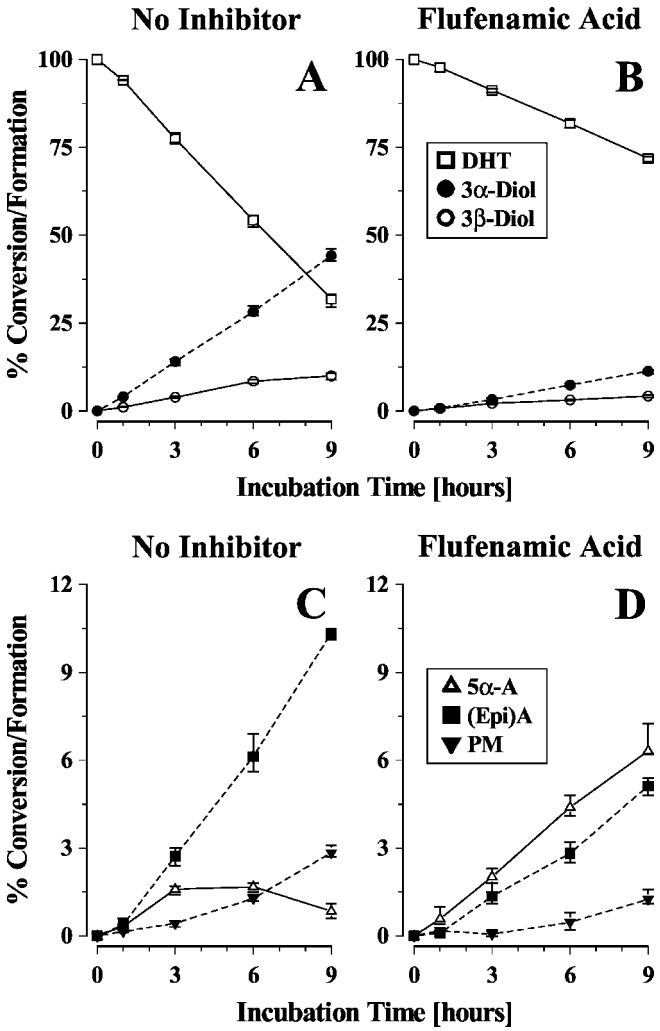

FIG. 9. **Inhibition of time-dependent 3α-/3β-HSD activity in HepG2 cells by the NSAID flufenamic acid.** *Panel A*, conversion of (□) DHT (10 μM) into 3α-Diol (●) and 3β-Diol (○); *panel B*, conversion of (□) DHT (10 μM) into 3α-Diol (●) and 3β-Diol (○) in the presence of 100 μM flufenamic acid; *panel C*, conversion of DHT (10 μM) into androstanedione (■), (epi)androsterone (△), and unidentified polar metabolites (▼); *panel D*, conversion of DHT (10 μM) into androstanedione (■), (epi)androsterone (△), and unidentified polar metabolites (▼) in the presence of 100 μM flufenamic acid. Time points were taken at 1, 3, 6, and 9 h as described under "Experimental Procedures." The results represent mean values ± range of three parallel experiments each assayed in duplicate.

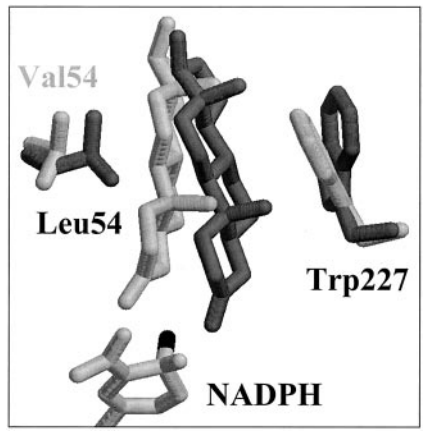

FIG. 10. **Binding modes for DHT in the active sites of AKR1C1 (*dark gray*) and AKR1C2 (*light gray*).** The preferred docking positions of DHT into binary complexes of AKR1C1-NADPH and AKR1C2-NADPH are shown by superimposition. A bent conformation of NADPH is shown. Details of docking simulations and PDB entry numbers are given under "Experimental Procedures." The pro-*R* hydrogen of NADPH (shown in *black*) is directed to the α-face of DHT in AKR1C1 (3β-HSD reaction) and to the β-face of the steroid in AKR1C2 (3α-HSD reaction).

the 3α[17β]-hydroxysteroid oxidase activity of the enzymes (34, 49). All enzymes demonstrated only very low 3β-hydroxysteroid oxidase activity, which indicates a clear stereo-selectivity of AKR1C2, AKR1C3, and AKR1C4 for 3α-hydroxysteroids in the oxidative direction.

The AKR1C isozymes worked efficiently either as NADPH-dependent 3-ketosteroid reductases or as NAD^+-dependent 3α[17β]-hydroxysteroid oxidases *in vitro*. In cells, the major reducing cofactor is NADPH and the major oxidative cofactor is NAD^+; in the cytosol, the [NADPH]/[$NADP^+$] ratio approaches 100:1, and the [NADH]/[NAD^+] ratios approaches 1:1000 (26, 27). Therefore, the *in vivo* direction of the AKR1C enzymes will be dictated by the ratio of reductive and oxidative cofactors. Two previous studies demonstrated that, in transfected COS-1 and PC-3 cell lines, AKR1C2 worked exclusively as a 3-ketosteroid reductase (46, 50). We showed that this is attributed to the fact that the NAD^+-dependent oxidation of 3α-Diol by homogeneous recombinant AKR1C2 is markedly inhibited by low micromolar concentrations of NADPH (46). Consequently, we determined the effect of opposing cofactors on the 3-ketosteroid reductase and 3α[17β]-hydroxysteroid oxidase activities of all AKR1C isoforms. The present data show that all AKR1C isoforms have their *in vitro* oxidase activity inhibited by low micromolar NADPH concentrations, whereas their *in vitro* reductase activity is not inhibited by NAD^+ (Fig. 7). The potent inhibition of the NAD^+-dependent oxidase reactions by low micromolar concentrations of NADPH suggests that *in vivo* the reductive activity will prevail unless the cellular redox balance is disturbed. Thus, AKR1C isoforms will reduce DHT to 3α- and 3β-Diol, but it is unlikely that the reverse reaction can occur *in vivo*.

The fact that, *in vitro*, the AKR1C enzymes showed 3α- and 3β-HSD activity raised the question whether these reactions also take place *in vivo*. HepG2 cells lack 3β-HSD/KSI mRNA expression but express substantial amounts of AKR1C1–AKR1C3 mRNA (Fig. 8). These cells were shown to reduce DHT into 3α- and 3β-Diol, and both reactions were inhibited by flufenamic acid (Fig. 9), which clearly indicates that the reduction of DHT in HepG2 cells is AKR1C-dependent. Consequently, our results provide direct evidence for the *in vivo* significance of the 3α/3β-HSD activities of the AKR1C enzymes.

To explain why AKR1C1–AKR1C4 can invert their stereochemical preference and catalyze the formation of 3α- as well as 3β-hydroxysteroids structure function relationships were considered. In terms of DHT reduction, the striking catalytic differences between the exceptionally homologous AKR1C1 and AKR1C2 isoforms are of special interest. The proteins differ in total by seven amino acids, and only one amino acid in their binding pockets is different (Leu-54 in AKR1C1 is Val-54 in AKR1C2). The small divergence in the binding pocket was thought to explain previously known functional differences of the two enzymes in that AKR1C1 prefers reactions at the C20 position and has a K_d for ursodeoxycholate 300-fold higher than AKR1C2 (35, 51). The difference in the binding pocket must also explain why AKR1C1 reduces DHT predominantly to 3β-Diol, whereas AKR1C2 catalyzes mainly the formation of 3α-Diol. Crystal structures of AKR1C1 and AKR1C2 showed that the NADP(H) cofactor binds in a highly conserved site with the nicotinamide ring orientated so that the 4-*pro*-R hydrogen is always transferred from the A-face and its C4 position is locked

relative to the catalytic tetrad (35–37). Therefore, functional plasticity of the isoforms relies on binding the steroid substrates in different orientations.

Computational simulations of the docking of DHT into AKR1C1 and AKR1C2 elucidated important differences in the orientation of DHT in the active sites of the two enzymes. The results fully explain the observed differences in stereo-specificity of the two enzymes (Fig. 10). The dimensions of the lateral chain of Leu-54/Val-54 dictate the preferred orientation of the steroid in the binding cavities. The preferred position of DHT docked into AKR1C2 is oriented for the 3α-HSD reaction. Because of steric hindrance created by the bulky Leu-54 side chain, such an orientation is not permitted for AKR1C1. By contrast, the preferred position of DHT docked into AKR1C1 is oriented for the 3β-HSD reaction because the A-ring of the steroid has swung to present its α-face to the nicotinamide ring for hydride transfer. In this position the 3β-HSD reaction can occur because sufficient proximity is maintained between the C3-ketone and the residues of the catalytic tetrad.

Our findings reveal a new picture of the functions of the human AKR1C isoforms in steroid hormone metabolism and action. Identification of the enzyme(s) responsible for the formation of 3β-tetrahydrosteroids was of special interest, because these steroids are not inert. 3β-Diol is an endogenous ligand for the estrogen receptor β, exerting, *e.g.*, anti-proliferative and apoptotic effects in prostate epithelial cells (52, 53). AKR1C1 catalyzes the conversion of DHT mainly into 3β-Diol. The enzyme is also known as human 20α-HSD and catalyzes effectively the reductive inactivation of progesterone to yield 20α-hydroxyprogesterone (34, 54). One might speculate that the enzyme acts simultaneously as an activator of pro-apoptotic estrogenic cell responses and as an inactivator of proliferative progestogenic cell responses. Detailed analyses of the expression levels of AKR1C1 in steroid hormone-dependent diseases, *e.g.* benign prostatic hyperplasia, prostate cancer, endometriosis, endometrial cancer, and mammary carcinoma based on disease stage and nuclear receptor status, is now warranted.

AKR1C2 acts as a stereo-selective and highly efficient reductive 3α-HSD. Therefore, the function of this enzyme may have to be redefined. Its function could well be the inactivation of DHT in peripheral tissues. A cytosolic enzyme responsible for the metabolic inactivation of DHT to prevent excessive activation of the cytosolic androgen receptor appears to be logical. For prereceptor regulation of steroid hormone action in androgen target tissues, AKR1C2 would work in an opposing direction to an SDR, which would furnish microsomal oxidative 3α-HSD activity (55, 56). This idea of an cytosolic reductive inactivating 3α-HSD and an microsomal oxidative activating 3α-HSD provides a switch for appropriate intracellular DHT concentrations to activate the androgen receptor. Down-regulation of AKR1C2 in androgen-dependent prostate cancer would be rational to achieve higher DHT concentrations, whereas unchanged or up-regulated expression of the enzyme would be rational to contribute to androgen-independent prostate cancer. In previous studies both trends were described (46, 50), but neither of the two studies determined the androgen receptor status as a control for hormone dependence of the tumor.

AKR1C3 showed only weak 3-ketosteroid reductase activity. Consequently, it appears unlikely that the isoform plays a major role in 3-ketosteroid metabolism. However, the enzyme is also known as 17β-HSD type 5 and exerts strong 17β-HSD activity (34, 49, 57). Consequently, it might instead function as a 17-ketosteroid reductase in peripheral steroid hormone target tissues catalyzing the intracrine activation of weak 17-ketosteroids into potent 17β-hydroxysteroids, *e.g.* androstenedione into testosterone and estrone into 17β-estradiol.

AKR1C4 is highly liver-specific, whereas mRNA expression of the other three isozymes was observed in a variety of human tissues displaying tissue-specific patterns (34). The function of AKR1C4 is most likely the catabolic inactivation of circulating Δ^4-3-ketosteroids in the liver. There, it works in concert with 5α/5β-reductases leading to the formation of 3α- and 3β-tetrahydrosteroids that are known to be glucuronidated or sulfated and finally eliminated (21, 22). This hypothesis is corroborated by the present study, which demonstrates a lack of stereoselectivity of AKR1C4 in the reductive direction and irreversible epimerization of 3α- to 3β-Diol because of negligible oxidation of 3β-Diol by AKR1C4. The epimerization of 3α-tetrahydrosteroids via the 3-ketosteroid intermediates offers a new route to 3β-tetrahydrosteroids and might provide an important pathway for irreversible conversion of circulating 3α-Diol to yield complete catabolic inactivation of androgens in human liver.

The observed differences in stereo-selectivity of the AKR1C isoforms might also play an important role in the regulation of neuroactive tetrahydrosteroids. 3α-Tetrahydrosteroids like allopregnanolone or 3α-Diol are potent positive allosteric mediators of the ionotropic γ-aminobutyric acid type A ($GABA_A$) receptor (58–60). As a consequence, they exhibit anesthetic, analgesic, anxiolytic, and anticonvulsant effects in a stereoselective manner. Their actions are not shared by the respective 3β-diastereomers. Instead, 3β-tetrahydrosteroids are potent antagonists of 3α-tetrahydrosteroids at the $GABA_A$ receptor (61–64). AKR1C1–AKR1C3 are expressed in the human brain, and AKR1C2 is believed to be responsible for the intracrine formation of neuroactive 3α-tetrahydrosteroids (65–70). The present study demonstrates that AKR1C1 has to be considered a possible source for the intracrine formation of 3β-tetrahydrosteroids within the central nervous system.

REFERENCES

1. Simard, J., Durocher, F., Mébarki, F., Turgeon, C., Sanchez, R., Labrie, Y., Couet, J., Trudel, C., Rhéaume, E., Morel, Y., Luu-The, V., and Labrie, F. (1996) *J. Endocr.* **150,** S189–S207
2. Penning, T. M. (1997) *Endocr. Rev.* **18,** 281–305
3. Jacobi, G. H., and Wilson, J. D. (1977) *J. Clin. Endocrinol. Metab.* **44,** 107–115
4. Stewart, M. E., Pochi, P. E., Strauss, J. S., Wotiz, H. H., and Clark, S. J. (1977) *J. Endocrinol.* **72,** 385–390
5. Wright, F., and Giacomini, M. (1980) *J. Steroid Biochem.* **13,** 639–643
6. Kinoshita, Y. (1981) *Endocrinol. Japon.* **28,** 499–513
7. Clair, P., Patricot, M. C., Mathian, B., and Revol, A. (1984) *J. Steroid Biochem.* **20,** 377–381
8. Trapp, T., Tunn, S., and Krieg, M. (1992) *J. Steroid Biochem. Mol. Biol.* **42,** 321–327
9. Pirog, E. C., and Collins, D. C. (1999) *J. Clin. Endocrinol. Metab.* **84,** 3217–3221
10. Jin, Y., and Penning, T. M. (2001) *Best Practice Res. Clin. Endocrin. Metab.* **15,** 79–94
11. van Doorn, E. J., Burns, B., Wood, D., Bird, C. E., and Clark, A. F. (1975) *J. Steroid Biochem.* **6,** 1549–1554
12. Saartok, T., Dahlberg, E., and Gustafsson, J.-Å. (1984) *Endocrinology* **114,** 2100–2106
13. Becker, H., Grabosch, E., Hoffmann, C., and Voigt, K. D. (1973) *Acta Endocrinol.* **73,** 407–416
14. Horst, H.-J., Dennis, M., Kaufmann, J., and Voigt, K. D. (1975) *Acta Endocrinol.* **79,** 394–402
15. Krieg, M., Horst, H.-J., and Sterba, M.-L. (1975) *J. Endocrinol.* **64,** 529–538
16. Kao, L. W. L., Lloret, A. P., and Weisz, J. (1977) *J. Steroid Biochem.* **8,** 1109–1115
17. Stenstad, P., and Eik-Nes, K. B. (1981) *Biochim. Biophys. Acta* **663,** 169–176
18. Morfin, R. F., di Stefano, S., Charles, J.-F., and Floch, H. H. (1977) *Biochimie* (*Paris*) **59,** 637–644
19. Offner, P., Sousa, R. L., Vena, R. L., Krinsky-Feibush, P., and LeQuesne, P. W. (1983) *J. Steroid Biochem.* **18,** 415–423
20. Gemzik, B., Jacob, S., Jennings, S., Veltman, J., and Parkinson, A. (1992) *Arch. Biochem. Biophys.* **296,** 374–383
21. Mauvais-Jarvis, P., and Baulieu, E.-E. (1965) *J. Clin. Endocr.* **25,** 1167–1178
22. Habrioux, G., Desfosses, B., Condom, R., Faure, B., and Jayle, M.-F. (1978) *Steroids* **32,** 61–71
23. Thomas, J. L., Strickler, R. C., Myers, R. P., and Covey, D. F. (1992) *Biochemistry* **31,** 5522–5527
24. Lorence, M., Murry, B. A., Trant, J. M., and Mason, J. I. (1990) *Endocrinology* **126,** 2493–2498
25. Rhéaume, E., Lachance, Y., Zhao, H.-F., Breton, N., Dumont, M., de Launoit, Y., Trudel, C., Luu-The, V., Simard, J., and Labrie, F. (1991) *Mol. Endocrinol.* **5,** 1147–1157

26. Krebs, H. A. (1973) *Symp. Soc. Exp. Biol.* **27,** 299–318
27. Reich, J. G., and Sel'kov, E. E. (1981) *Energy Metabolism of the Cell: A Theoretical Treatise*, Academic Press, New York
28. Wang, J., Chai, X., Eriksson, U., and Napoli, J. L. (1999) *Biochem. J.* **338,** 23–27
29. Gough, W. H., VanOoteghem, S., Sint, T., and Kedishvili, N. Y. (1998) *J. Biol. Chem.* **273,** 19778–19785
30. Biswas, M. G., and Russell, D. W. (1997) *J. Biol. Chem.* **272,** 15959–15966
31. Chetyrkin, S. V., Hu, J., Gough, W. H., Dumaual, N., and Kedishvili, N. Y. (2001) *Arch. Biochem. Biophys.* **386,** 1–10
32. Chetyrkin, S. V., Belyaeva, O. V., Gough, W. H., and Kedishvili, N. Y. (2001) *J. Biol. Chem.* **276,** 22278–22286
33. He, X.-Y., Merz, G., Yang, Y.-Z., Pullakart, R., Mehta, P., Schulz, H., and Yang, S.-Y. (2000) *Biochim. Biophys. Acta* **1484,** 267–277
34. Penning, T. M., Burczynski, M. E., Jez, J. M., Hung, C.-F., Lin, H.-K., Ma, H., Moore, M., Palackal, N., and Ratnam, K. (2000) *Biochem. J.* **351,** 67–77
35. Jin, Y., Stayrook, S. E., Albert, R. H., Palackal, N. T., Penning, T. M., and Lewis, M. (2001) *Biochemistry* **40,** 10161–10168
36. Nahoum, V., Gangloff, A., Legrand, P., Zhu, D. W., Cantin, L., Zhorov, B. S., Luu-The, V., Labrie, F., Breton, R., and Lin, S. X. (2001) *J. Biol. Chem.* **276,** 42091–42098
37. Couture, J.-F., Legrand, P., Cantin, L., Luu-The, V., Labrie, F., and Breton, R. (2003) *J. Mol. Biol.* **331,** 593–604
38. Burczynski, M. E., Harvey, R. G., and Penning, T. M. (1998) *Biochemistry* **37,** 6781–6790
39. Ratnam, K., Ma, H., and Penning, T. M. (1999) *Biochemistry* **38,** 7856–7864
40. Bradford, M. M. (1976) *Anal. Biochem.* **72,** 248–254
41. Pawlowski, J. E., and Penning, T. M. (1994) *J. Biol. Chem.* **269,** 13502–13510
42. Gingras, S., and Simard, J. (1999) *Endocrinology* **140,** 4573–4584
43. Morris, G. M., Goodsell, D. S., Halliday, R. S., Huey, R., Hart, W. E., Belew, R. K., and Olson, A. J. (1998) *J. Comput. Chem.* **19,** 1639–1662
44. Penning, T. M., and Talalay, P. (1983) *Proc. Natl. Acad. Sci. U. S. A.* **80,** 4504–4508
45. Wilkinson, G. N. (1961) *Biochem. J.* **80,** 324–332
46. Rižner, T., Lin, H. K., Peehl, D. M., Steckelbroeck, S., Bauman, D. R., and Penning, T. M. (2003) *Endocrinology* **144,** 2922–2932
47. Talalay, P., and Levy, H. R. (1959) *The Steric and Molecular Specificity of Steroid Dehydrogenases (Ciba Foundation Study Group No. 2, Ciba Foundation)* pp. 53–78, Little, Brown and Co., Boston
48. Huang, X.-F., and Luu-The, V. (2000) *J. Biol. Chem.* **275,** 29452–29457
49. Lin, H.-K., Jez, J. M., Schlegel, B. P., Peehl, D. M., Pachter, J. A., and Penning, T. M. (1997) *Mol. Endocrinol.* **11,** 1971–1984
50. Ji, Q., Chang, L., VanDenBerg, D., Stanczyk, F. Z., and Stolz, A. (2003) *Prostate* **54,** 275–289
51. Matsuura, K., Deyashiki, Y., Sato, K., Ishida, N., Miwa, G., and Hara, A. (1997) *Biochem. J.* **323,** 61–64
52. Weihua, Z., Mäkelä, S., Andersson, L. C., Salmi, S., Saji, S., Webster, J. I., Jensen, E. V., Nilsson, S., Warner, M., and Gustafsson, J.-Å. (2001) *Proc. Natl. Acad. Sci.* **98,** 6330–6335
53. Weihua, Z., Lathe, R., Warner, M., and Gustafsson, J.-Å. (2002) *Proc. Natl. Acad. Sci.* **99,** 13589–13594
54. Zhang, Y., Dufort, I., Rheault, P., and Luu-The, V. (2000) *J. Mol. Endocrinol.* **25,** 221–228
55. Walsh, P. C., and Wilson, J. D. (1976) *J. Clin. Invest.* **57,** 1093–1097
56. Shaw, G., Renfree, M. B., Leihy, M. W., Shackleton, C. H. L., Roitman, E., and Wilson, J. D. (2000) *Proc. Natl. Acad. Sci.* **97,** 12256–12259
57. Dufort, I., Rheault, P., Huang, X.-F., Soucy, P., and Luu-The, V. (1999) *Endocrinology* **140,** 568–574
58. Paul, S. E., and Purdy, R. H. (1992) *FASEB J.* **6,** 2311–2322
59. Rupprecht, R., and Holsboer, F. (1999) *Trends Neurosci.* **22,** 410–416
60. Lambert, J. J., Belelli, D., Harney, S. C., Peters, J. A., and Frenguelli, B. G. (2001) *Brain Res. Rev.* **37,** 68–80
61. Prince, R. J., and Simmonds, M. A. (1992) *Neurosci. Lett.* **135,** 273–275
62. Maitra, R., and Reynolds, J. N. (1998) *Can. J. Physiol. Pharmacol.* **76,** 909–920
63. Wang, M. D., Backstrom, T., and Landgren, S. (2000) *Acta Physiol. Scand.* **169,** 333–341
64. Wang, M., He, Y., Eisenmann, L. N., Fields, C., Zheng, C.-M., Mathews, J., Benz, A., Zorumski, E., Steinbach, J. H., Covey, D. F., Zorumski, C. F., and Mennerik, S. (2002) *J. Neurosci.* **22,** 3366–3375
65. Steckelbroeck, S., Watzka, M., Reichelt, R., Hans, V. H. J., Stoffel-Wagner, B., Heidrich, D. D., Schramm, J., Bidlingmaier, F., and Klingmüller, D. (2001) *J. Clin. Endocrinol. Metab.* **86,** 1324–1331
66. Steckelbroeck, S., Watzka, M., Stoffel-Wagner, B., Hans, V. H. J., Lioba, R., Clusmann, H., Elger, C. E., Bidlingmaier, F., and Klingmüller, D. (2001) *Mol. Cell. Endocrinol.* **171,** 165–168
67. Trauger, J. W., Jiang, A., Stearns, B. A., and LoGrasso, P. V. (2002) *Biochemistry* **41,** 13451–13459
68. Usami, N., Yamamoto, T., Shintani, S., Higaki, Y., Ishikura, S., Katagiri, Y., and Hara, A. (2002) *Biol. Pharm. Bull.* **25,** 441–445
69. Stoffel-Wagner, B., Watzka, M., Steckelbroeck, S., Ludwig, M., Clusmann, H., Bidlingmaier, F., Casarosa, E., Luisi, S., Elger, C. E., and Beyenburg, S. (2003) *Epilepsy Res.* **54,** 11–19
70. Higaki, Y., Usami, N., Shintani, S., Ishikura, S., El-Kabbani, O., and Hara, A. (2003) *Chem. Biol. Interact.* **143/144,** 503–513

Human Cytosolic 3α-Hydroxysteroid Dehydrogenases of the Aldo-keto Reductase Superfamily Display Significant 3 β-Hydroxysteroid Dehydrogenase Activity: IMPLICATIONS FOR STEROID HORMONE METABOLISM AND ACTION

Stephan Steckelbroeck, Yi Jin, Sridhar Gopishetty, Busola Oyesanmi and Trevor M. Penning

J. Biol. Chem. 2004, 279:10784-10795.
doi: 10.1074/jbc.M313308200 originally published online December 12, 2003
